ISSN 1674-1056
http://cpb.iphy.ac.cn
http://iopscience.iop.org/cpb
中国物理 B
Chinese Physics
中国物理 Chinese Physics B

The effect of dislocations on the thermodynamic properties of Ta single crystal under high pressure by molecular dynamics simulation

Yalin Li(李亚林), Jun Cai(蔡军), Dan Mo(莫丹), Yandong Wang(王沿东)

Citation: Chin. Phys. B . 2018, 27(8): 086401. **doi:** 10.1088/1674-1056/27/8/086401

Journal homepage: http://cpb.iphy.ac.cn; http://iopscience.iop.org/cpb

What follows is a list of articles you may be interested in

Anomalous behavior and phase transformation of *α* -GaOOH nanocrystals under static compression

Zhao Zhang(张钊), Hang Cui(崔航), Da-Peng Yang(杨大鹏), Jian Zhang(张剑), Shun-Xi Tang(汤顺熙), Si Wu(吴思), Qi-Liang Cui(崔啟良)

Chin. Phys. B . 2017, 26(10): 106402. **doi:** 10.1088/1674-1056/26/10/106402

Secondary relaxation and dynamic heterogeneity in metallic glasses: A brief review

J C Qiao(乔吉超), Q Wang, D Crespo, Y Yang(杨勇), J M Pelletier

Chin. Phys. B . 2017, 26(1): 016402. **doi:** 10.1088/1674-1056/26/1/016402

Effect of fluorine groups and different terminal chains on the electro-isomerization of azobenzene liquid crystals

Jing-Jing Xiong(熊晶晶), Dong Shen(沈冬), Zhi-Gang Zheng(郑致刚), Xiao-Qian Wang(王骁乾)

Chin. Phys. B . 2016, 25(9): 096401. **doi:** 10.1088/1674-1056/25/9/096401

Photo-induced athermal phase transitions of Hg*X* (*X*= S, Se, Te) by *ab initio* study

Da-hua Ren(任达华), Xin-lu Cheng(程新路), Hong Zhang(张红)

Chin. Phys. B . 2016, 25(7): 076401. **doi:** 10.1088/1674-1056/25/7/076401

Numerical modeling of condensate droplet on superhydrophobic nanoarrays using the lattice Boltzmann method

Qing-Yu Zhang(张庆宇), Dong-Ke Sun(孙东科), You-Fa Zhang(张友法), Ming-Fang Zhu(朱鸣芳)

Chin. Phys. B . 2016, 25(6): 066401. **doi:** 10.1088/1674-1056/25/6/066401

The effect of dislocations on the thermodynamic properties of Ta single crystal under high pressure by molecular dynamics simulation*

Yalin Li(李亚林)[1], Jun Cai(蔡军)[1,†], Dan Mo(莫丹)[1], and Yandong Wang(王沿东)[2]

[1] School of Nuclear Science & Engineering, North China Electric Power University (NCEPU), Beijing 102206, China
[2] State Key Laboratory for Advanced Metal Materials, University of Science & Technology Beijing, Beijing 100083, China

(Received 19 April 2018; revised manuscript received 31 May 2018; published online 10 July 2018)

The thermodynamic properties of Ta metal under high pressure are studied by molecular dynamics simulation. For dislocation-free Ta crystal, all the thermodynamic properties considered are in good agreement with the results from experiments or higher level calculations. If dislocations are included in the Ta crystal, it is found that as the dislocation density increases, the hydrostatic pressure at the phase transition point of bcc→hcp and hcp→fcc decreases, while the Hugoniot temperature increases. Meanwhile, the impact pressure at the elastic–plastic transition point is found to depend on the crystallographic orientation of the pressure. As the dislocation density increases, the pressure of the elastic–plastic transition point decreases rapidly at the initial stage, then gradually decreases with the increase of the dislocation density.

Keywords: Ta, high pressure, phase transition, dislocation density, molecular dynamics (MD)

PACS: 64.30.Ef, 61.50.Ks, 64.70.K, 64.70.kd **DOI:** 10.1088/1674-1056/27/8/086401

1. Introduction

The phase transition of Ta metal under high pressure is a hot research topic at present.[1–12] Ta is a bcc structure under the standard condition, but the phase transition of the crystal under high pressure and high temperature is very complex, thus it has been extensively studied. Hsiung and Lassila found that Ta transformed from the bcc structure to the hcp structure by the impact test of 45 GPa.[13,14] The studies of Brown and Shaner[15] showed that Ta melted under the impact pressure of around 300 GPa. However, other impact experiments showed that the bcc structure of Ta remained stable when the shock pressure reached 500 GPa.[16–21] In the theoretical aspects, Ravelo *et al.* found an elastic–plastic transformation of the Ta crystal in the pressure range of 40 GPa–55 GPa by molecular dynamics simulation, and the phase transformed from bcc structure to hcp structure under the hydrostatic pressure of 463 GPa.[22] Burakovsky *et al.* found that the structure of fcc was more stable than that of bcc when the hydrostatic pressure was higher than 150 GPa by the density functional theory (DFT) method.[23] On the other hand, the DAC static pressure experiment showed that the bcc structure of Ta remained stable up to 174 GPa. Although the physical properties of Ta under high temperature and high pressure have been extensively investigated, as far as we know, no one has studied the effects of dislocations on the thermodynamic properties of metals under high pressure. However, the dislocations play a major role in the phase transformation and mechanical properties of metals. Therefore, this article aims to explore the effects of dislocations on the physical properties of Ta metals under high pressure by the molecular dynamics method.

2. Theory and method

A variety of atomic interaction potentials have been proposed for metal Ta,[24–32] and the embedded atom potential proposed by Ravelo and Germann is used in the present work.[22] Under zero pressure, the metal Ta has a bcc structure, and the theoretical lattice constant, cohesive $E_{\rm cho}$, the elastic constants C_{11}, C_{12}, and C_{44} are 3.304 Å, −8.1 eV/atom, 263 GPa, 161 GPa, and 82 GPa, respectively. When we calculate the elastic constants, the X, Y, and Z axes of the computational unit cell are taken along ⟨100⟩, ⟨010⟩, ⟨001⟩ crystallographic directions, respectively. The unit cell has the size of 132.16 Å ×132.16 Å ×132.16 Å and contains 1.28×10^5 atoms. The periodic boundary condition is applied to the computational unit cell along the X, Y, and Z directions. In order to study the effect of dislocations on physical properties of the material, computational unit cells containing different dislocation densities are built. The dislocation formed in this work is a common 1/2⟨110⟩ {112} edge dislocation in bcc crystals.

3. Results and discussions

3.1. Physical characteristics under hydrostatic pressure

In this work, the physical properties of Ta bcc structure under high hydrostatic pressure are first calculated.

*Project supported by the National Natural Science Foundation of China (Grant No. 51231002) and the Basic Scientific Research Projects in Central Colleges and Universities (Grant No. 2018ZD10).

†Corresponding author. E-mail: caijun@ncepu.edu.cn

© 2018 Chinese Physical Society and IOP Publishing Ltd

The sound velocity was obtained by the Voigt–Reuss–Hill approximation.[33] The bulk modulus B and the shear modulus G of a cubic crystal can be obtained based on the following formula

$$G = \frac{G_{\rm V} + G_{\rm R}}{2}, \tag{1}$$

$$B = \frac{C_{11} + 2C_{12}}{3}, \tag{2}$$

where

$$G_{\rm V} = \frac{C_{11} - C_{12} + 3C_{44}}{5}, \tag{3}$$

$$G_{\rm R} = \frac{5(C_{11} - C_{12})C_{44}}{4C_{44} + 3(C_{11} - C_{12})}. \tag{4}$$

In the above formulas, C_{11}, C_{12}, and C_{44} are the elastic constants of Ta crystal with bcc structure. The longitudinal sound velocity $C_{\rm L}$ and the bulk sound velocity $C_{\rm B}$ can be calculated as

$$C_{\rm L} = \sqrt{\frac{B + 4\,G/3}{\rho}}, \tag{5}$$

$$C_{\rm B} = \sqrt{\frac{B}{\rho}}. \tag{6}$$

The calculated results of elastic constants, sound velocity, and enthalpy of Ta with bcc, fcc, and hcp structures are shown in Figs. 1(a), 1(b), and 1(c), respectively, as a function of the hydrostatic pressure. As can be seen from Figs. 1(a) and 1(b), under zero pressure, the elastic constants C_{11}, C_{12}, C_{44}, bulk modulus B, and shear modulus G are 263 GPa, 161 GPa, 82 GPa, 195 GPa, and 68 GPa, respectively, which agree well with the experimental values.[21,34] From Fig. 1(a) it is found that shear modulus G, the elastic constants C_{11}, and C_{12} increase with the increase of the hydrostatic pressure, while bulk modulus B and elastic constant C_{44} increase initially and then decrease at the pressure over 350 GPa. As the pressure continues to increase, B, C_{11}, and C_{12} show a discontinuous change around the pressure of 450 GPa, which indicates that the bcc structure of Ta crystal remains stable up to the pressure of 450 GPa. For pressure than higher 450 GPa, the bcc structure of Ta crystal transforms into the hcp structure, as shown below. The sound velocities $C_{\rm L}$ and $C_{\rm B}$ of Ta crystal are also calculated to be 4.13 km/s and 3.81 km/s at zero pressure and increase with the increase of hydrostatic pressure. A discontinuous variation of the sound velocities $C_{\rm L}$ and $C_{\rm B}$ are also found around the pressure of 450 GPa, as shown in Fig. 1(b). These results agree well with the ones from higher level calculations of Orlikowski *et al.*[35] It also supports the conclusion that a phase transformation from the bcc structure of Ta to hcp structure occurs at the hydrostatic pressure of about 450 GPa. Note that the discontinuous change seems to be observed in the variation of C_{44} and G versus pressure, as shown in Fig. 1(a). This may be due to the fact that the magnitude in discontinuous change of C_{44} and G at the point of the phase transition is vanishingly small compared with the corresponding C_{11}, C_{12}, B, C_{44}, and G.

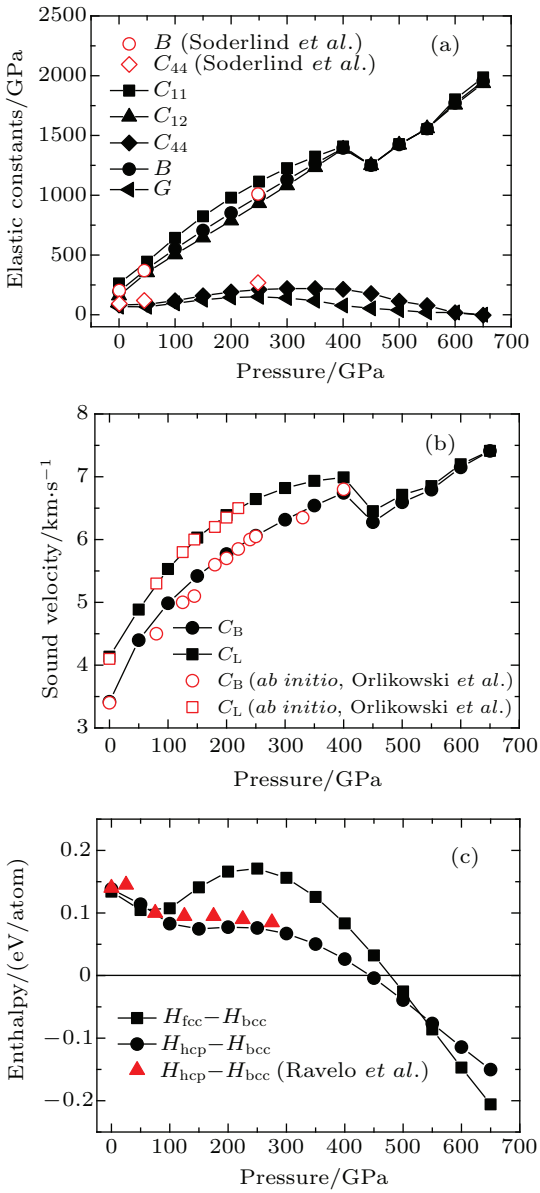


Fig. 1. (color online) (a) The elastic constants, (b) sound velocity, and (c) the enthalpy difference between fcc/hcp and bcc structure of Ta as a function of the hydrostatic pressure.

Figure 1(c) shows the variation of enthalpy versus hydrostatic pressure under the condition of zero temperature for Ta crystal with fcc and hcp structures. The enthalpy values are based on the bcc structure as a reference point. As seen in the figure, at the pressure below 450 GPa, the enthalpy is the smallest for bcc structure, second for hcp structure, and the largest for fcc structure. When the pressure is more than 450 GPa, the enthalpy of the Ta crystal with hcp structure becomes the smallest. When the hydrostatic pressure continues to increase to 530 GPa, the fcc structure possesses the smallest enthalpy, while the enthalpy of hcp structure is in the middle, and the enthalpy of the bcc structure is the largest. This indi-

cates that the crystal Ta with bcc structure is most stable below 450 GPa. When the pressure is higher than 450 GPa, the bcc structure first transforms into hcp structure. This result is in good agreement with the result by Ravelo *et al.*,[22] which predicted that the crystal Ta with bcc structure transformed into hcp structure at the pressure of about 463 GPa. If the pressure is further increased to more than 530 GPa, the hcp structure will change to the fcc structure, as shown in Fig. 1(c).

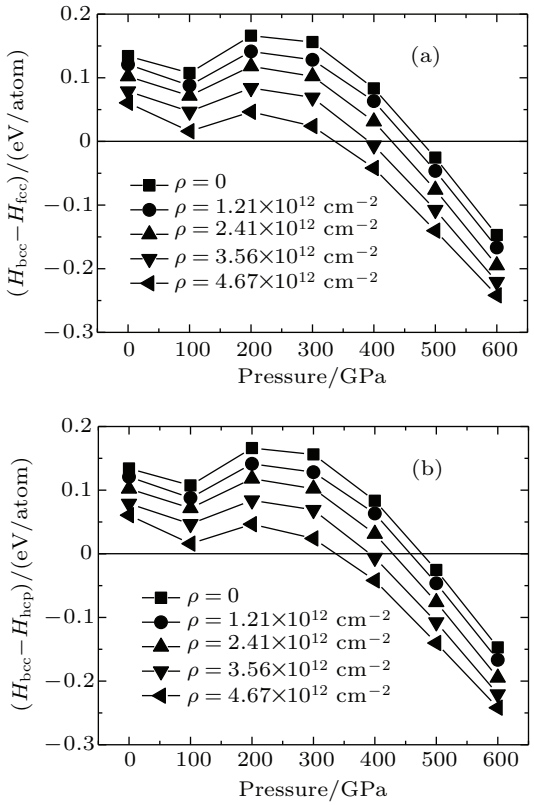


Fig. 2. The enthalpy difference (a) between bcc structure and fcc structure, and (b) between bcc structure and hcp structure, as a function of pressure under different dislocation densities.

When dislocations are present in crystals, they might produce stress among atoms, so the crystals become less stable than a perfect crystal. Thus a phase transition from bcc to hcp may be more prone to take place under high pressure in this situation. Figures 2(a) and 2(b) show the enthalpy difference between bcc and fcc structure of Ta crystal, and between bcc and hcp structure, respectively. As shown in Fig. 2, when the bcc structure is dislocation-free, the transition pressure of bcc→fcc is found to be about 478 GPa, and the corresponding pressure of bcc→hcp transition is about 450 GPa. From the figure it can be seen that the presence of dislocation seriously affects the phase transition pressure of bcc→fcc and of bcc→hcp. For instance, at the dislocation density $\rho = 4.67 \times 10^{12}$ cm^{-2}, the phase transition pressures of the bcc→fcc and bcc→hcp drop to 345 GPa and 90 GPa, respectively. These values are far smaller than the ones of the phase transition in the defect-free Ta crystal. It can also be seen from Fig. 2 that the phase transition pressures of bcc→fcc and bcc→hcp of Ta crystal decrease with the increase of the dislocation density.

3.2. Physical characteristics under impact pressure

Figure 3 illustrates the variation of the sound velocity U_S versus the particles velocity U_P under the impact pressure along different crystallographic directions of ⟨100⟩, ⟨110⟩, and ⟨111⟩. As shown in Figs. 3(a)–3(c), for defect-free Ta single crystal, all shock directions exhibit high Hugoniot elastic limits. For instance, when the impact pressure is applied to the crystallographic orientation ⟨100⟩, the variation of the sound velocity with respect to the particle velocity presents a discontinuity at 60 GPa with an elastic strain of 14.9%. This shows that when the impact pressure is less

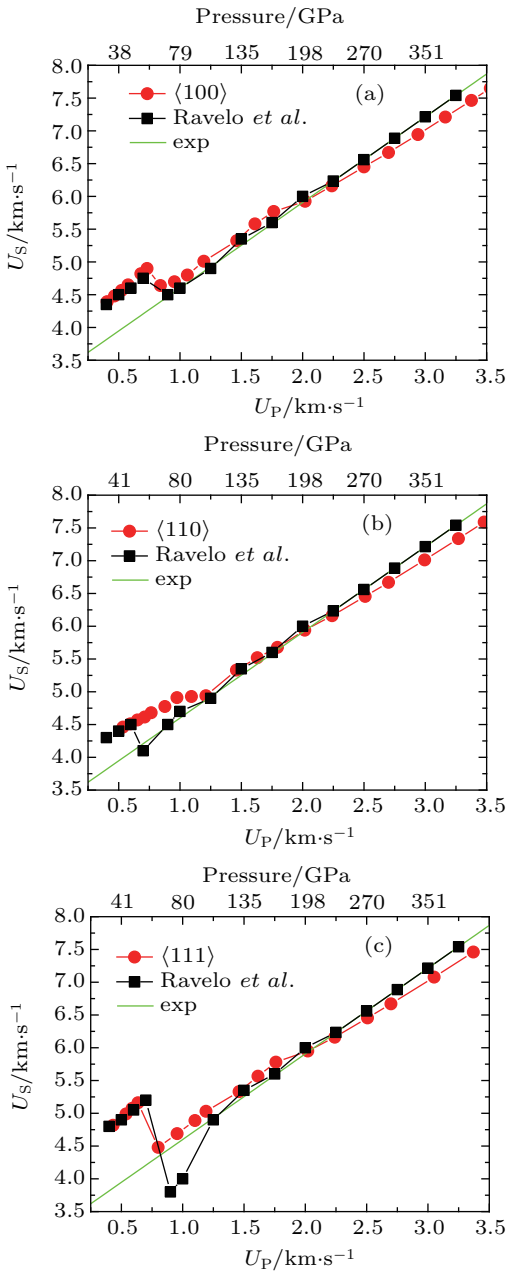


Fig. 3. (color online) The variation of sound velocity U_S versus the particle velocity U_P under different impact pressures along the crystallographic orientation of (a) ⟨100⟩, (b) ⟨110⟩, and (c) ⟨111⟩.

than 60 GPa, the crystal is elastically deformed; when the impact pressure is greater than 60 GPa, the crystal is plastically deformed. For the crystallographic orientations of ⟨110⟩ and ⟨111⟩, this discontinuity occurs at 85 GPa and 55 GPa, respectively, and the corresponding elastic strain limits are 20% and 12.3%, respectively. In the work of Ravelo *et al.*,[22] the Ta crystal was found to undergo an elastic–plastic transition in the 40 GPa–55 GPa range with the corresponding elastic strain of 10%–14%. Present numerical results are basically consistent with the ones by Ravelo *et al.*[22] and experiments.[17]

We also calculate the shock pressure at the elastic–plastic transition point as a function of the dislocation density, and the results are shown in Fig. 4. The shock pressure is applied to Ta crystal along ⟨100⟩, ⟨110⟩, and ⟨111⟩ crystallographic directions. It is found that the pressure at the elastic–plastic transition point decreases rapidly with the increase of the dislocation density when the density is smaller than 1×10^{12} cm^{-2}, and then gradually decreases. When the dislocation density ρ increases to about 9×10^{12} cm^{-2}, the shock pressure at the elastic–plastic transition point decreases to 30 GPa, 37.5 GPa, and 31 GPa along ⟨100⟩, ⟨110⟩, and ⟨111⟩ crystallographic directions, respectively.

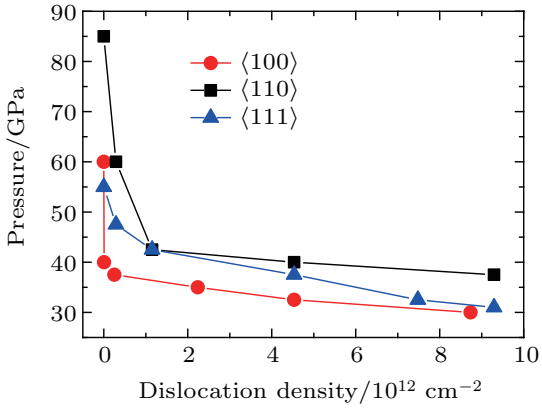


Fig. 4. (color online) The variation of the shock pressure versus dislocation density ρ at the elastic–plastic transition point along ⟨100⟩, ⟨110⟩, and ⟨111⟩ crystallographic directions.

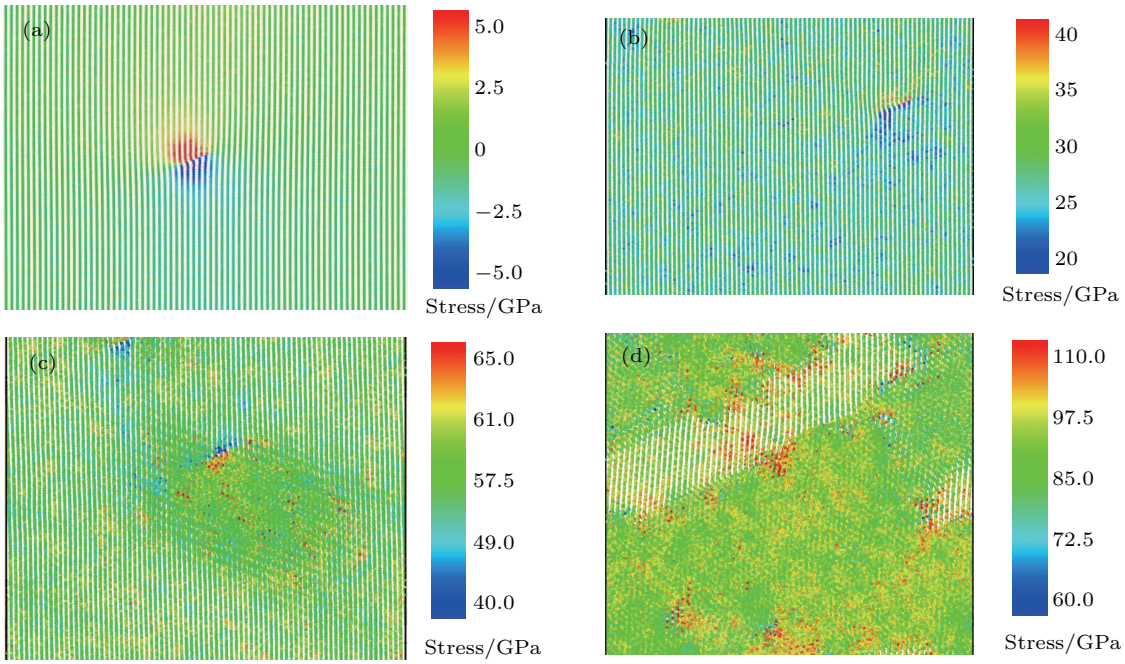


Fig. 5. (color online) Atomic arrangement and stress distribution with atomic resolutions, where a Ta crystal including a 1/2⟨110⟩ {112} edge dislocation (the corresponding density $\rho = 0.29 \times 10^{12}$ cm^{-2}) is impacted under the pressure of 100 GPa at different moments of (a) $t = 0$ ps, (b) $t = 5$ ps, (c) $t = 10$ ps, and (d) $t = 30$ ps. The shock pressure is along the ⟨110⟩ crystallographic direction.

As an example, figure 5 shows the atomic arrangement and stress distribution of a Ta crystal including a 1/2⟨110⟩ {112} edge dislocation (the corresponding density $\rho = 0.29 \times 10^{12}$ cm^{-2}) with atomic resolutions. The crystal is subjected to the pressure of 100 GPa at different moments of 0 ps, 5 ps, 10 ps, and 30 ps. The shock pressure is applied along the ⟨110⟩ crystallographic direction. In these panels, the horizontal axis is along the ⟨110⟩ crystallographic direction toward the right of the sheet, the vertical axis is along the $\langle \bar{1}11 \rangle$ crystallographic direction upward to the top of the sheet, and the third axis is along the $\langle 1\bar{1}2 \rangle$ crystallographic direction perpendicular to the plane of the sheet. As shown in Figs. 5(a) and 5(b), the dislocations are located at the region with larger stress gradient, i.e., the dislocation is near the central position of the crystal in Fig. 5(a) and the upper right corner of the crystal in Fig. 5(b). It can also be seen in Fig. 5(a) that a compression stress area is formed in the upper part of the crystal over the dislocation core and a tensile stress area is created in the lower part of the crystal below the dislocation core. This is a typical characteristic of stress distribution for an edge dislocation in fcc metal. From the figure it can be seen that within the initial 5 ps, the shock pressure forces the dislocation at the

center of the crystal to move to the position of the upper right corner of the crystal by slipping and climbing. Figures 5(c) and 5(d) show that more and more regions of the larger stress gradient are produced with continuous shocking on the crystal, which indicates that more and more dislocations are generated, thus the plastic deformation spreads to a wider region with the elasped time. These dislocations produce stress fields and then enhance the effect on the mechanical properties of the crystals.

Figure 6 shows the Hugoniot curve of the Ta crystals. As can be seen from the figure, the calculated Hugoniot temperature increases with the increase of the pressure for the dislocation-free Ta crystal under the shock pressure along the ⟨100⟩ direction. This is in line with the results by first principle calculations[36] and molecular dynamics simulations.[29] As shown in Fig. 6, the upper curve is the Hugoniot curve of the Ta crystal with larger dislocation density, the middle curve is for the smaller concentration of dislocations, and the lower curve is for dislocation-free Ta crystal. This indicates that the Hugoniot temperature increases obviously with the increase of the dislocation density in the Ta crystal. A similar phenomenon is also found in these Ta crystals under the shock pressure along ⟨110⟩ and ⟨111⟩ directions, and is not shown here.

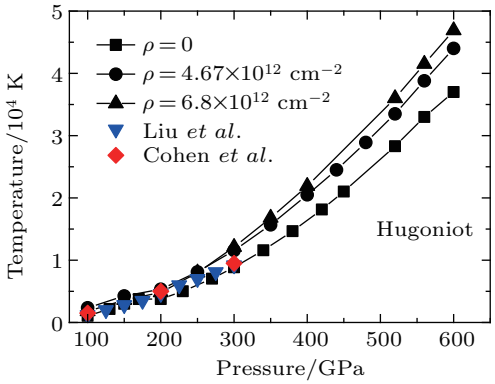


Fig. 6. (color online) The curves of temperatures of Ta crystal along the Hugoniot path, where the shock pressure is applied along the ⟨100⟩ crystallographic direction.

4. Conclusion

In this paper, the physical properties of crystal Ta under the hydrostatic and impact pressure, such as enthalpy, elastic constants, sound velocity, and so on are calculated by molecular dynamics. Under hydrostatic pressure, it is found that the bcc structure of defect-free Ta crystal is the most stable when the pressure is smaller than 450 GPa. As the pressure further increases, a phase transition takes place from the bcc structure of the defect-free Ta crystal to its hcp structure. When the pressure continues to increase to 530 GPa, the hcp structure of the defect-free Ta crystal transforms into fcc structure. If dislocations of crystals are taken into account, the pressure at the phase transition point will decrease with the increase of the dislocation density. The impact pressure at the elastic–plastic transition point depends on the crystallographic directions along which the impact pressure is loaded. The impact pressure of the defect-free Ta crystal at the elastic–plastic transformation points along the ⟨100⟩, ⟨110⟩, and ⟨111⟩ direction is found to be 60 GPa, 85 GPa, and 55 GPa, respectively. As the dislocation density ρ increases, the impact pressure at the elastic–plastic transition point decreases, while the Hugoniot temperature is found to increase.

Acknowledgment

We would like to thank Mr. Wajahat Afsar from the School of Nuclear Science and Engineering of NCEPU for his help in reading the manuscript and correcting it.

References

[1] Li Y H, Chang J Z, Li X M and Zhang L 2012 *Chin. Phys. Lett.* **29** 046201
[2] Pang W W, Zhang P, Zhang G C and Xu A G 2015 *Sci. Rep.* **4** 3628
[3] Zhang P L, Gong Z Z, Ji G F, *et al.* 2013 *Chin. Phys. Lett.* **30** 066401
[4] Ming L C and Manghnani M H 1978 *J. Appl. Phys.* **49** 208
[5] Xu J, Mao H K and Bell P M 1984 *High Temp. High Press.* **16** 495
[6] Cynn H and Yoo C S 1999 *Phys. Rev. B* **59** 8526
[7] Errandonea D, Schwager B and Ditz R 2001 *Phys. Rev. B* **63** 132104
[8] Santamaría Pérez D, Ross M, Errandonea D, *et al.* 2009 *J. Chem. Phys.* **130** 124509
[9] Burakovsky L, Preston D L and Silbar R R 2000 *J. Appl. Phys.* **88** 6294
[10] Mukherjee S, Cohen R E and Gülseren O 2003 *J. Phys.: Condens. Matter* **15** 855
[11] Ross M, Boehler R and Japel S 2006 *J. Phys. Chem. Solids* **67** 2178
[12] Verma A K, Rao R S, Godwal B K 2004 *J. Phys.: Condens. Matter* **16** 4799
[13] Hsiung L M and Lassila D H 1998 *Scr. Mater.* **38** 1371
[14] Hsiung L M and Lassila D H 1998 *Scr. Mater.* **39** 603
[15] Brown J M and Shaner J W 1984 *Shock Waves in Condens. Matter* (Amsterdam: Elsevier) p. 91
[16] Holmes N C, Moriarty J A, Gathers G R and Nellis W J 1989 *J. Appl. Phys.* **66** 2962
[17] Mitchell A C and Nellis W J 1981 *J. Appl. Phys.* **52** 3363
[18] Nellis W J, Mitchell A C and Young D A 2003 *J. Appl. Phys.* **93** 304
[19] Moriarty J A, Belak J F, Rudd R E, Soderlind P, Streitz F H and Yang L H 2002 *J. Phys.: Condens. Matter* **14** 2825
[20] Moriarty J A 1994 *Phys. Rev. B* **49** 12431
[21] Soderlind P and Moriarty J A 1998 *Phys. Rev. B* **57** 10340
[22] Ravelo R, Germann T C, Guerrero O, An Q and Holian B L 2013 *Phys. Rev. B* **88** 134101
[23] Burakovsky L, Chen S P, Preston D L, Belonoshko A B, Rosengren A, Mikhaylushkin A S, Simak S I and Moriarty J A 2010 *Phys. Rev. Lett.* **104** 255702
[24] Johnson R A and Oh D J 1989 *J. Mater. Res.* **4** 1195
[25] Guellil A M and Adams J B 1992 *J. Mater. Res.* **7** 639
[26] Finnis M W and Sinclair J E 1984 *Philos. Mag. A* **50** 45
[27] Ackl, G J and Thetford R 1987 *Philos. Mag. A* **56** 15
[28] Dai X D, Kong Y, Li J H and Liu B X 2006 *J. Phys.: Condens. Matter* **18** 4527
[29] Liu Z L, Cai L C, Chen X R and Jing F Q 2008 *Phys. Rev. B* **77** 024103
[30] Lee B J, Baskes M I, Kim H and Cho Y K 2001 *Phys. Rev. B* **64** 184102
[31] Mishin Y and Lozovoi A Y 2006 *Acta Mater.* **54** 5013
[32] Moriarty J A, Benedict L X, Glosli J N, Hood R Q, Orlikowski D A, Patel M A, Söderlind P, Streitz F H, Tang M and Yang L H 2006 *J. Mater. Res.* **21** 563
[33] Hill R 1952 *Proc. Phys. Soc. A* **65** 349
[34] Katahara K W, Manghnani M H and Fisher E S 1979 *J. Phys. F* **9** 773
[35] Orlikowski D, Söderlind P and Moriarty J A 2006 *Phys. Rev. B* **74** 054109
[36] Cohen R E and Gülseren O *Phys. Rev. B* **63** 224101